

EdgeSoil 2.0 – Soil Analyzer Using Convolutional Neural Network and Camera Imaging for Agricultural Robotics

Roni Kasemi¹, Lara Lammer², Stefan Thalhammer³ and Markus Vincze²

Abstract—Soil is the most important building element of agriculture and its analysis is crucial for healthy plants and a high crop yield. But apart from its importance, soil analysis is a tedious and time-consuming task. This paper presents EdgeSoil 2.0, a non-invasive, accurate, and real-time robotic system for soil pH prediction, a key parameter of soil status for farmers. The EdgeSoil 2.0 predicts the pH value of the soil in real-time, using a live video stream from a webcam with an average of 7 FPS. The method is suitable to be implemented on edge devices necessary for the application: we are using a mobile robot with the NVIDIA Jetson Nano module which is running a pH-estimator trained with a Convolutional Neural Network (CNN) on a novel dataset we built for this purpose. Predictions are performed while the robot is moving over the plowed field before the planting process starts. In order to achieve the best performance, we train the pH-estimator with different input modalities and validate each result using Mean Squared Error (MSE) and Standard Deviation (SD). We are able to achieve accurate results with the MSE value of 0.08, the SD value of 0.15, and with testing results from the field showing up to ± 0.3 deviation from the GT value during prediction, which is sufficient to comply with agricultural standards.

I. INTRODUCTION

Soil analysis is crucial for ensuring crop health and maximizing crop yield, which are directly affected by soil parameters, such as pH, nitrogen, phosphorus, and potassium levels [1][2]. The challenge is that due to the tedious collection of soil samples and the time-consuming laboratory analysis, soil analysis is rarely carried out before sowing. [3].

Diverse robotic systems have been proposed for performing tasks such as weed detection [4], plant disease classification [5], and fruit monitoring [6], [7], [8]. As compared to these tasks, soil analysis presents a considerable challenge since exhaustive analysis of soil parameters requires sophisticated environmental measurements or laboratory equipment [10], [11], [12], [13], [14], [15], [16], [17]. In [10] and [11] a continuous internet connection is assumed to correlate measurements with vast amounts of data on climatic parameters, satellite images, and mean annual temperatures, to name a few. This is especially challenging in rural areas and emerging countries since these environmental parameters are not always available. Methods for directly performing soil analysis are thus preferred. The works presented in [16]

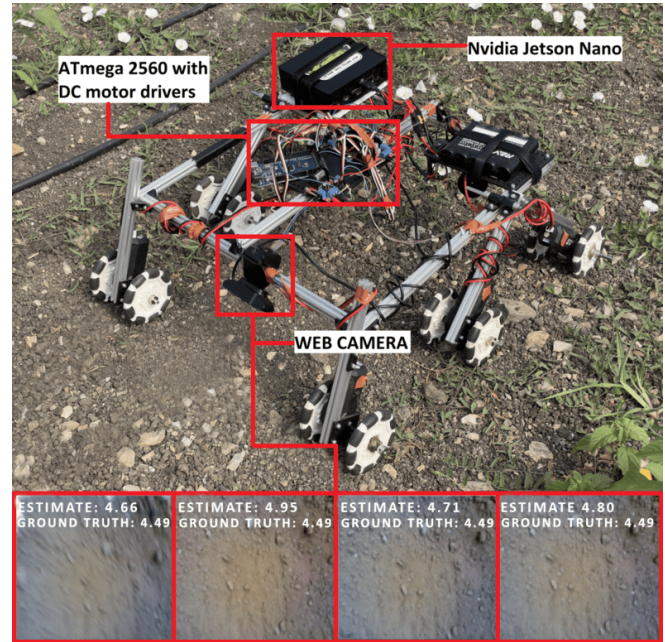


Fig. 1. **EdgeSoil 2.0** Presented is a cost-efficient mobile platform for performing online pH level analysis. At the bottom, frames and corresponding estimated pH-level, captured and processed in real time, are visualized.

and [17] use time-consuming drilling mechanisms to collect soil samples, which in turn are analyzed in a laboratory. Similar approaches rely on measuring diverse soil parameters: the amount of organic soil matter [12], temperature and humidity [13], CO₂ levels [14], and electrical resistivity [15]. As compared to these works, this paper focuses on analyzing the soil's pH value, because it is one of the most important parameters and therefore has been termed the "master soil variable" by environmental soil science experts [1].

In this paper, we investigate the observability of the pH value in RGB images and present a modular edge device for predicting soil pH levels. Our findings confirm the findings of [18] that the soil's pH value correlates with the RGB image's saturation. Based on this confirmation, we have built EdgeSoil 2.0 as the continuation of our previous work EdgeSoil [19], which presented a robotic system for the task of classifying the soil type. Here we present a system to obtain the pH value using a custom-tailored CNN architecture that allows us to exploit the soil RGB images alongside the mean saturation value of those images in order to increase the performance of the CNN. Using a novel dataset and a custom-tailored CNN, we train a pH-estimator, which predicts the pH value of the soil in real-time

*This work was not supported by any organization

¹Roni Kasemi is with the Faculty of Mechatronics Engineering, UBT College, 10000 Prishtina, Kosovo roni.kasemi@ubt-uni.net

²Lara Lammer and Markus Vincze, are with the Faculty of Electrical Engineering and Information Technology, TU Wien, 1040 Vienna, Austria {lammer, vincze}@acin.tuwien.ac.at

³Stefan Thalhammer is with Industrial Engineering Department, UAS Technikum Vienna, 1040 Vienna, Austria thalhammer@technikum-wien.at

without the need for an internet connection or depending on vast amounts of data, thus being suitable for farmers in emerging countries and also eliminating the laborious and time-consuming process of soil sample collection and laboratory analysis. The contributions of EdgeSoil 2.0 are listed as follows:

- Real-time and accurate pH-measuring robotic system with 97% of the predictions resulting below a threshold of 0.5 deviation of the ground truth pH value. The robotic system uses solely RGB images, which require no internet connection or databases.
- We identify a correlation between mean saturation values of soil images of agricultural land and the respective pH value of the soil. Using the mean saturation value as additional input to the pH-estimator leads to an error reduction of 68.5%, as compared to only using RGB.
- A novel dataset with soil images and their pH values from laboratory tests¹.

The paper proceeds as follows. Section 2 includes the related work and two different approaches used regarding soil analysis. Section 3 explains our approach and the method used to implement it. Section 4 presents the dataset, how it is created, and what combinations of data are included. Section 5 discusses the evaluation and the achieved results. Section 6 summarises the findings and indicates future directions of work.

II. RELATED WORK

There are two main approaches used to analyze soil parameters, which are soil analysis using a) vast amounts of data collected from systems like GIS and satellite imagery, and b) sensor data and soil samples directly from the field.

Regarding the first type of approach, Felegari et al. [10] tackle the soil analysis problem by predicting total soil nitrogen using three machine-learning techniques. Instead of using any kind of robot or collecting soil images, the authors use different types of data like climate parameters, satellite data, topographic components, and soil samples. Using these data from different zones, they trained three different models using a Support Vector Machine, Boosted Regression Tree, and Random Forest algorithms. After validating each model using mean absolute error, root mean square error, and coefficient of determination, they concluded that Random Forest and Boosted Regression Tree algorithms were most successful in predicting total soil nitrogen value. A similar approach was used by Pham et al. [11] who also tried to estimate soil organic carbon, total nitrogen, and soil reaction values by using different environmental variables like land use and topographic wetness index. In this case, the authors used regression kriging and ordinary kriging methods for prediction, by concluding that the regression kriging method was more precise compared to others. The common point of these approaches and our paper is to analyze soil parameters, even though the used methodologies are totally different from

ours since we do not depend on outside data and use our pH-estimator for prediction.

Regarding the second type of approaches, Zhou et al. [12] focus on mapping soil organic matter using drones to collect multi-spectral images and obtaining nine parameters out of the collected images, from which the parameter $NLI_{rededge2}$ highly correlated with soil organic matter. After training with different models, the authors concluded that the random forest algorithm produced the best results when validated with coefficient of determination, root mean square error, mean bias error, and the ratio of performance to inter-quartile distance. A similar approach to ours was done by Iqbal et al. [13] who developed a mobile robot to analyze both soil and plant parameters. The robot is equipped with a depth camera to analyze the morphological traits of a plant and a manipulator with a sensor to detect the temperature and humidity of the soil. Another robotic system that analyzes a very specific soil parameter, soil respiration, was done by Jaffe et al. [14] who emphasizes that this parameter is important in agriculture but usually overlooked. The robot uses an arm-like mechanism that holds sensors for measuring temperature, humidity, and CO₂ levels from the top of the soil, which after being measured are sent to the NVIDIA Jetson board via a radio module for further processing. Ünal et al. [15] also use a mobile robot, which uses Wenner four-probe measurement method to determine the electrical resistivity (ER) of the soil in real time and store that information in a database. Besides measurement with different sensors, mobile robots are used also in soil sample collection [16][17] by including here other information such as location, satellite images of the field, and atmospheric conditions which are collected and sent to cloud storage.

The work closest to this paper was conducted by Barman and Choudhury [18] who experimented with the correlation between soil pH values and the saturation of the soil images. The authors collected a total of 120 soil samples and 120 soil images in the laboratory, with a white background in order to extract the soil colors better. Then they proceeded to extract the saturation value of each soil image and the pH value of each soil sample, thus running the correlation analysis between those parameters, and they found out that these two values are highly correlated (0.859) with the pH values of the soil. While this study was conducted in the laboratory, we introduce a dataset from fields and show that images from fields at different times and conditions can be analyzed to obtain the pH value. The dataset contains images both from the agricultural land and laboratory conditions, thus creating a diverse mix dataset, since we found that lighting conditions drastically change the final prediction results and the lighting in the terrain is not the same as in the laboratory. Also, we run the correlation test on a much larger dataset with 4800 images, which gives us a better estimate and valuation.

III. EDGESOIL 2.0 - METHOD FOR pH VALUE ESTIMATION

To estimate the pH value only from images taken on the field, we propose the EdgeSoil 2.0 approach. An advantage is

¹<https://www.kaggle.com/datasets/ronikasemi/blackredmix>

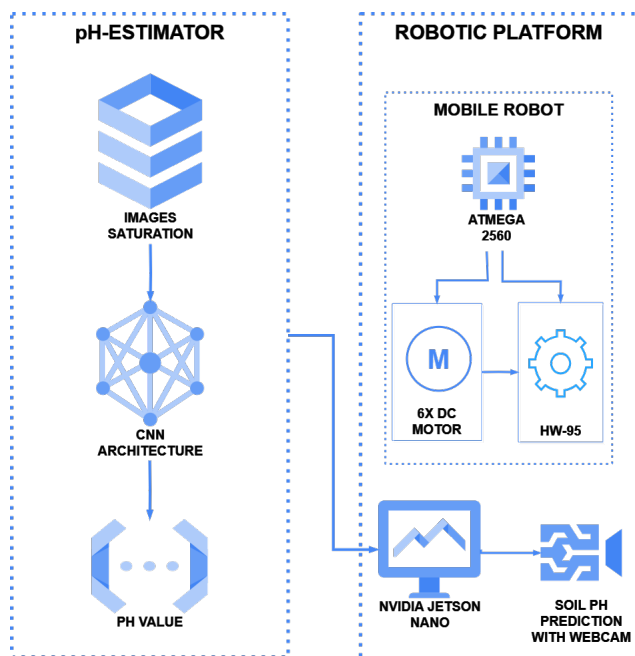


Fig. 2. **System Diagram.** Two main building blocks of EdgeSoil 2.0, with a platform including the mobile robot and NVIDIA Jetson Nano, which runs the pH-estimator trained from CNN.

that it is tailored to run on edge devices in farmland including developing countries where constant internet connection cannot be assured. EdgeSoil 2.0 consists of two main building blocks with the purpose of eliminating the time-consuming and laborious process of soil pH analysis, without depending on an internet connection or any other database (see Figure 2). The first building block consists of the pH-estimator trained with CNN which is responsible for estimating the pH level of the soil by using only the RGB images collected from the webcam. The second building block consists of the robotic platform which includes the mobile robot and the Nvidia Jetson Nano² equipped with a webcam and running the pH-estimator, as an embedded device carried from the robot. The whole system is composed of easily available and low-cost components thus making it easily reproducible by researchers and practitioners. Compared to contemporary work it is easily available to the community and as such also in emerging countries.

pH-estimator. Since our main objective is to predict the soil pH value only from images and given previous works [20][21], a Convolutional Neural Network architecture is well suited for developing the predictive model. The idea behind this approach is that using an efficient CNN model running on the NVIDIA Jetson Nano is a perfect trade-off between the processing time and the capacity of the model. Furthermore, as an edge device, the NVIDIA Jetson Nano specializes in solving image processing tasks, which is perfect for using a CNN on it.

In order to fulfill our task, we developed a CNN architecture (see Figure 3) with common components such as convolutional layers, dense layers, batch normalization, and

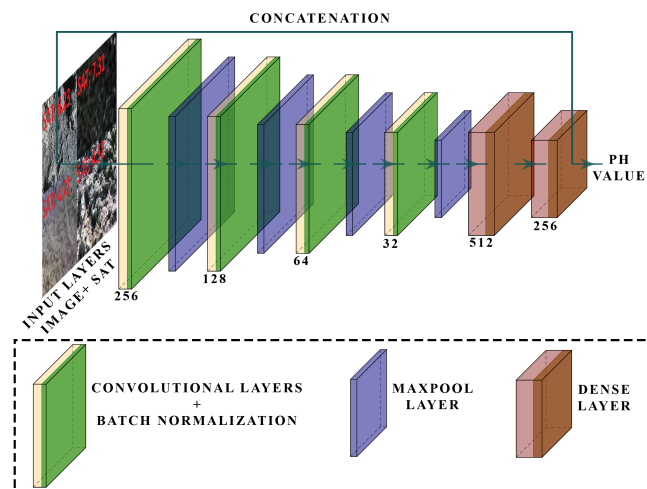


Fig. 3. **pH-estimator.** CNN architecture for training the pH-estimator: it contains six layers with the input layer consisting of the RGB soil images and their mean saturation value.

max pooling layers. The CNN contains four convolutional layers with filter sizes of 32, 64, 128, and 256. Training is supervised using MSE loss. Following the convolutional layers are two dense layers with 512 and 256 neurons, each of them followed by batch normalization and max pooling layers. Besides those layers, our CNN architecture contains L2 regularization of 0.001, data augmentation, dropout of 0.5, learning rate adjustment of 0.001, Mean Squared Error as loss function supervising the training, and early stopping.

What differentiates our architecture from the traditional CNN is the dual input layer, since the traditional CNN architectures [20] usually only uses images as input data. In our case, we additionally pass the mean saturation of the corresponding soil image, and the RGB image itself to the network. Also, what makes our architecture specific is the concatenation feature [22], which concatenates the scalar mean saturation input with the output of the last dense layer (see Figure 3).

Robotic Platform. The mobile robot is a six-wheeled model with enough traction power and flexibility to navigate easily on many different types of fields. For navigation, the robot uses a simple yet effective method [19] by calculating the distance with integrated encoders on the DC motors thus covering the field in vertical lines. The main control unit for reading the encoder data and moving the robot via HW-95 motor drivers is the ATmega2560 microcontroller³, which is sufficient to perform those tasks, and also it is low-cost which is a great advantage for using it in less developed countries. While the robot is moving in the field, it is performing the pH prediction by using the webcam shown in Figure 1 and in real time by synchronizing the speed of the robot movement and processed frames per second (see Figure 7). The prediction is made from the pH-estimator running on NVIDIA Jetson Nano, which is powerful enough to run such a model, and yet it is very compact in size and power management which makes it very practical to be carried from any mobile robot.

²<https://developer.NVIDIA.com/embedded/jetson-nano-developer-kit>

³<https://www.microchip.com/en-us/product/atmega2560>



Fig. 4. **Data Collection.** The two top red boxes show the areas where soil data was collected. On the bottom of the image are five different fields, with a total of 5.6 hectares, where soil images and samples are collected.

IV. DATASET FOR EDGESOIL 2.0

The focus of EdgeSoil 2.0 is to predict the pH level of the soil just by using soil RGB images obtained from real-time video streaming from a webcam mounted on the agricultural robot and in order to design such a system, data collection is crucial. Since there is no existing data for such a task, we created a novel dataset including the RGB soil images and the ground truth (GT) which is the pH value measured for each collected soil sample in the laboratory. Furthermore, we make the created dataset publicly available in order to be easily accessible to researchers and practitioners.

For images and soil sample collection, we chose a specific area in Southeast Europe, which has three types of soil - black, brown, and red - thus giving us diversity in soil types and pH values. In five different locations, as shown in Figure 4, we collected a total of 25,000 images, but also in each location, we collected four soil samples from different spots on that location, thus having 20 soil samples in total. Because the soil images are taken on the same day and time, the created dataset is biased regarding lighting conditions. To overcome this, we collected soil RGB images again from the soil samples in different lighting conditions simulated inside the laboratory and mixed the dataset with the original images taken from the field in order to create a more diverse dataset for training the pH-estimator.

The importance of the lighting comes from the research findings of Barman [18] who states that the correlation coefficient is high between the saturation values of soil images and the pH value of those soil samples. Therefore, a diverse dataset in terms of lighting is very important, since it will impact drastically those image parameters, and as such the correlation cannot be considered only with one

type of lighting condition. Besides the image collection, we measured the pH level of each soil sample with standard methodology [23] and labeled each sample with a measured value, thus creating the ground truth (GT) for the pH-estimator.

With the collected images, we created two different datasets named *BlackBrownRed* and *BlackRedMix*, each with different image content. The *BlackBrownRed* dataset includes brown-type soil images collected from the terrain lighting conditions and black and red-type soil images collected in the laboratory lighting conditions from the soil samples, with a total of 4800 images. The *BlackRedMix* includes only black and red type soil images, collected from terrain and laboratory lighting conditions, with a total of 3600 images. The reason why the number of images is less than the original 25,000 images collected is that after extensive experimentation, we observe that the same results are obtained with a much smaller number of images, thus speeding up the training process and producing a faster working model.

V. EXPERIMENTS AND EVALUATION

This section presents the correlation between soil pH values and the mean saturation of soil images since we want to confirm the findings of Barman and Choudhury [18] who concluded that saturation values of the soil images are highly correlated (0.895) with the pH values of the soil. Confirming and replicating those findings is important in order to use the mean saturation of soil images for performance improvement of the pH-estimator. Implementation results of the pH estimator follow, which we then evaluate in terms of the ability to estimate the pH values of RGB images in the test set.

A. Correlation between Image Parameters and the pH Value

In order to prove the association between soil pH value and the scalar parameters such as mean saturation and mean hue of the soil images we run the correlation test. The reason for this analysis is to find any related parameter with pH value, in order to enhance the CNN model by using it as an extra input layer. The Pearson correlation (r) [24] is used to measure the relationship between the mentioned scalar values and pH values of the soil, which is formulated as:

$$r = ((x_i - \hat{x})(y_i - \hat{y})) / (\sqrt{\sum (x_i - \hat{x})^2 * \sum (y_i - \hat{y})^2}) \quad (1)$$

where x_i and y_i are the individual data points, \hat{x} and \hat{y} are the means of the x and y variables, respectively.

We applied the correlation test for both *BlackRedMix* and *BlackBrownRed* datasets and the corresponding pH values of soil images on those datasets. The results show that there is a high correlation (0.8) between the mean saturation of images from the *BlackRedMix* dataset and pH values of the black and red type of soil, which also proves the findings in [18].

The results are shown in Figure 5 which are seen as two groups of data points with the upper data points representing the black type of soil with higher pH values, and lower data points representing the brown type of soil with lower pH

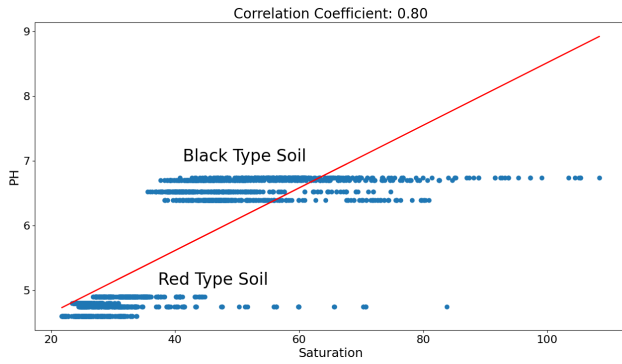


Fig. 5. **Correlation between Soil pH Values and Mean Saturation.** Correlation results tested on the *BlackRedMix* dataset. The two groupings of data points represent two types of soil, with the black type of soil having higher pH values and the red type of soil having lower pH values.

TABLE I

CORRELATION RESULTS BETWEEN pH VALUES OF THE SOIL AND M_S - MEAN SATURATION, M_H - MEAN HUE, M_R - MEAN RED, M_G - MEAN GREEN, AND M_B - MEAN BLUE PARAMETERS OF SOIL IMAGES.

	M_S	M_H	M_R	M_G	M_B
Correlation	0.80	-0.13	-0.31	-0.34	-0.36

values. Also, for each specific pH value on the Y axis, we have a range of corresponding mean saturation values on the X axis of the graph. This is happening since we have large numbers of soil images collected from each of the five fields (see Figure 4), and the pH value of the soil does not change if the soil type is the same. The reason for having a range of saturation values corresponding to the same pH value is that the dataset is created in different lighting conditions, so the image of the same soil is taken in different light intensities, different angles, and different distances, in order to create a diverse dataset and not be biased and dependent on the mentioned conditions. Since saturation is directly affected by those conditions [25], this causes a range of saturation values to exist for a given pH value. Based on the results, it is seen that with the increasing pH values of the soil, the mean saturation values of that soil image are also increasing.

Besides the saturation, we test if there is a correlation between soil pH values and other soil image parameters such as mean hue, mean red, mean green, and mean blue values of soil images (see Table I). We find no significant correlation between those values and thus continue with only the mean saturation value as extra input beside the image datasets for improving the performance of the pH-estimator.

B. Soil Analysis Evaluation

Building on the findings of the previous section, we evaluate the system for soil pH value analysis on an edge device. We present experiments demonstrating that the mean saturation value as additional input to our pH-estimator reduces the pH value regression error. In the following we conduct a runtime analysis and a real-world test run of EdgeSoil 2.0 on previously unseen agricultural land.

TABLE II

EVALUATION OF FOUR DIFFERENT OUTPUTS PRODUCED FROM THE COMBINATION DATASET AND INPUT MODALITIES RGB WITH/WITHOUT SATURATION, WITH THE MSE AND SD RESULTS FOR EACH OUTPUT.

Input	Dataset	MSE	SD
RGB	BlackBrownRed	0.26	0.26
	BlackRedMix	0.16	0.24
RGSB	BlackBrownRed	0.15	0.20
	BlackRedMix	0.08	0.15

1) *Implementation Details:* In order to achieve the best performance, we trained the pH-estimator with different input modalities and analyzed the results for each one. First, we split the dataset into 80% training and 20% testing, which is followed by data augmentation and normalization. Data augmentation includes rotation, shift, shear, zoom, and flipping, then each pixel intensity is normalized to a range of [0, 1]. Also, the soil images in the dataset are resized with a shape 300x300x3 before the training process starts.

RGB - Refers to using RGB images as input to the pH-estimator. For training, we test separately two datasets, *BlackBrownRed* and *BlackRedMix* with the first dataset taking 6 to 8 hours for training and the second one 5 to 6 hours.

RGSB - Refers to additionally pass the mean saturation value of each soil image, alongside the RGB images to the pH-estimator, since we proved that the pH value of soil and mean saturation of soil images are highly correlated (see Figure 5). The concatenation feature is implemented because the input is of a dual nature, and again two datasets are tested, with similar training time as mentioned above.

2) *pH-estimator Evaluation:* For the evaluation of four pH-estimators trained with different input combinations, we use Mean Squared Error (MSE) and Standard Deviation (SD) on a test set containing 720 soil images, which are the most suited evaluation techniques for regression models [26][27].

When we compare the evaluation results from four input modalities, the best results are obtained from the RGSB (see Table II) which uses the *BlackRedMix* dataset and mean saturation values of the soil images from the dataset as input for CNN architecture. We can see an improvement in MSE results for 68.5% with the passing of mean saturation value alongside the image dataset as an input. The improvement is also backed up by the high correlation coefficient (see Figure 5) between the mean saturation of soil images and the pH values of the soil, which shows that the pH values of soil increase with the increasing of the mean saturation values of soil images. The cause for this is the difference in color for each type of soil which directly affects the mean saturation of the soil image [25] thus resulting in a correlation between mean saturation and pH values of soil.

3) *Runtime Analysis:* We evaluate the runtime of EdgeSoil 2.0 by measuring the frames per second (FPS) that are processed during deployment. On average, the pH-estimator computing on the NVIDIA Jetson Nano achieves a seven FPS and performs 400 pH measurements in 52 seconds (see

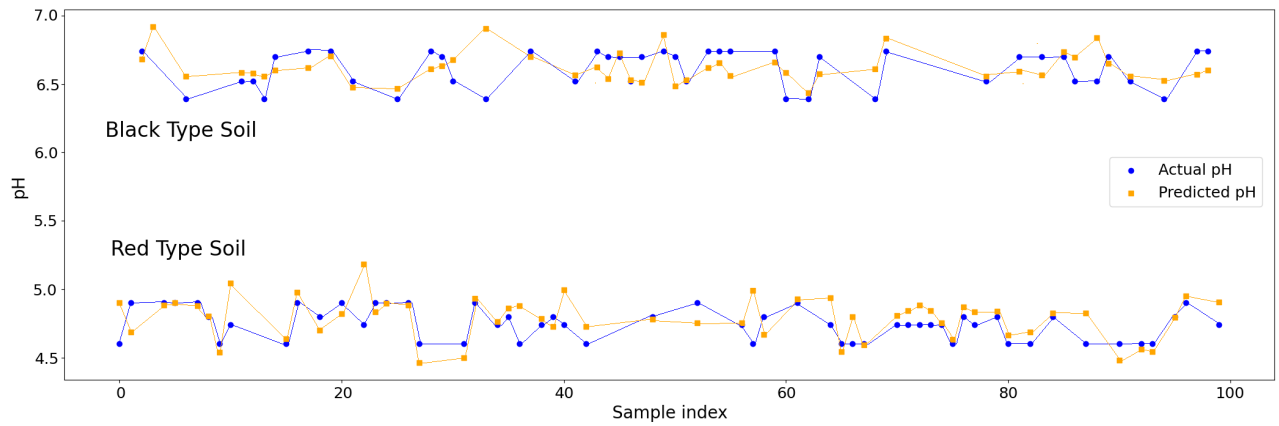


Fig. 6. **MSE Result of RGBS.** MSE evaluation results from the *BlackRedMix* dataset show actual pH values compared to predicted pH values from the pH-estimator for 100 data samples out of 720 in total.

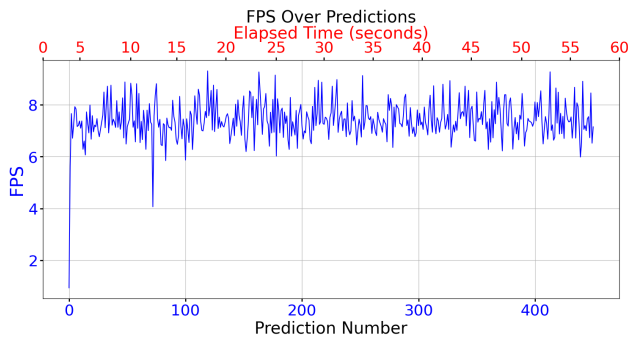


Fig. 7. **Runtime Evaluation of EdgeSoil 2.0.** Runtime evaluation shows that EdgeSoil 2.0 is running the video stream at an average of 7 FPS and is performing 400 pH predictions for less than a minute.

Figure 7). The frame rate and the number of measurements are sufficient to achieve the desired pH information since the aim is to collect the accurate pH value and not to increase the number of measurements per second.

4) *Real-world Experiments with EdgeSoil 2.0:* Besides the runtime performance, the EdgeSoil 2.0 is also tested in a real-world scenario. We present results on soil images captured outside the agricultural land used for the creation of the dataset. In both cases, for black and red types of soil, the deviation on pH value prediction maximally deviates with 0.3 from ground truth (see Figure 8). This deviation is considered a low error for agricultural standards [28]. This experiment provides a verification that the accuracy achieved on the test data transfers well to new data.

VI. CONCLUSION

In this paper, we present a non-invasive, accurate, and real-time pH soil measuring method using only RGB images from a mobile vehicle as used in agricultural robotics. The prediction is performed using the presented pH-estimator EdgeSoil 2.0 that runs on a NVIDIA Jetson Nano and is trained on CNN with input combinations of soil image dataset and the scalar values of mean saturation of each soil image. EdgeSoil 2.0 provides pH value estimates during operation at a rate of 7 Hz with only ± 0.3 deviations in pH value compared to ground truth. The validation results such

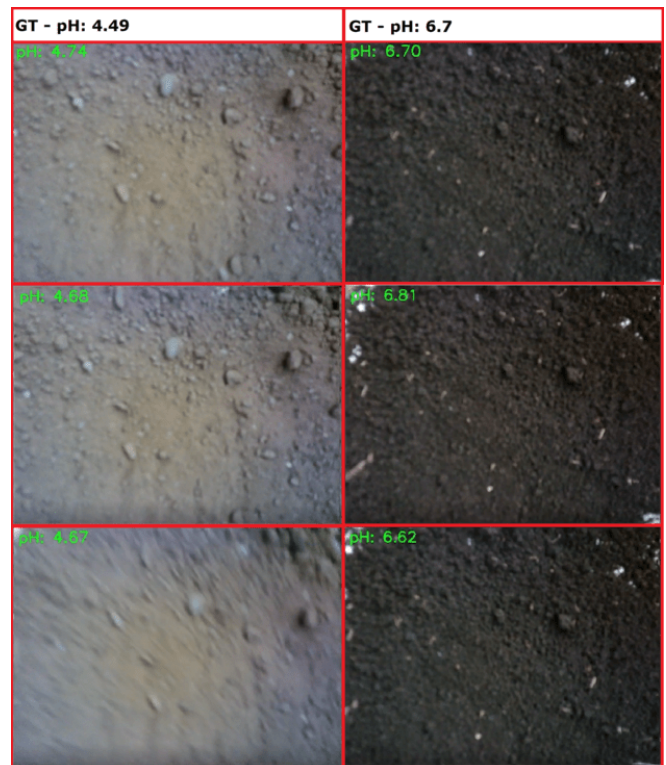


Fig. 8. **EdgeSoil 2.0 Performance of pH Prediction on Terrain.** EdgeSoil 2.0 performs soil pH prediction on the black and red types of soil on the terrain conditions. On the top left of each frame is shown the predicted pH value, which is compared to the GT value on the top.

as MSE 0.08 and SD 0.4 show that the model is accurate at the pH prediction task. These results have been achieved on a novel dataset that contains black and red types of soil, from five fields in Southeast Europe (Kosovo) and is available openly.⁴

Future work will investigate how to expand the pH prediction for more types of soil and also predict other soil parameters by using only machine vision, which would give the farmers better overall information about their land for optimal fertilization and crop growth and health.

⁴<https://www.kaggle.com/datasets/ronikasemi/blackredmix>

REFERENCES

- [1] Neina, D., 2019. The role of soil pH in plant nutrition and soil remediation. *Applied and environmental soil science*, 2019, pp.1-9.
- [2] Zhong, W., Gu, T., Wang, W., Zhang, B., Lin, X., Huang, Q. and Shen, W., 2010. The effects of mineral fertilizer and organic manure on soil microbial community and diversity. *Plant and soil*, 326, pp.511-522.
- [3] Kasemi, R., Lammer, L. and Vincze, M., 2022. The gap between technology and agriculture, barrier identification and potential solution analysis. *IFAC-Papers OnLine*, 55(39), pp.314-318.
- [4] Raffik, R., Mayukha, S., Hemchander, J., Abishek, D., Tharun, R. and Kumar, S.D., 2021, October. Autonomous Weeding Robot for Organic Farming Fields. In *2021 International Conference on Advancements in Electrical, Electronics, Communication, Computing and Automation (ICAECA)* (pp. 1-4). IEEE.
- [5] Karpyshev, P., Ilin, V., Kalinov, I., Petrovsky, A. and Tsetserukou, D., 2021, January. Autonomous mobile robot for apple plant disease detection based on cnn and multi-spectral vision system. In *2021 IEEE/SICE international symposium on system integration (SII)* (pp. 157-162). IEEE.
- [6] Doddamani, S.T., Karadgi, S. and Giriyaapur, A.C., 2022. Multi-Label Classification of Cotton Plant with Agriculture Mobile Robot. In *Data Intelligence and Cognitive Informatics: Proceedings of ICDICI 2021* (pp. 759-772). Singapore: Springer Nature Singapore.
- [7] Choi, T., Would, O., Salazar-Gomez, A. and Cielniak, G., 2022, May. Self-supervised representation learning for reliable robotic monitoring of fruit anomalies. In *2022 International Conference on Robotics and Automation (ICRA)* (pp. 2266-2272). IEEE.
- [8] Chen, Y., Lin, J., Du, X., Fang, B., Sun, F. and Li, S., 2022, May. Non-destructive fruit firmness evaluation using vision-based tactile information. In *2022 International Conference on Robotics and Automation (ICRA)* (pp. 2303-2309). IEEE.
- [9] Bini, D., Pamela, D. and Prince, S., 2020, March. Machine vision and machine learning for intelligent agrobots: A review. In *2020 5th International conference on devices, circuits and systems (ICDCS)* (pp. 12-16). IEEE.
- [10] Felegari, S., Moravej, K., Sharifi, A., Golchin, A. and Karami, P., 2023. Prediction of total soil nitrogen variations using three machine learning approaches and remote sensing data. Preprint available on Research Square, (<https://www.researchsquare.com/article/rs-2952425/v1>)
- [11] Gia Pham, T., Kappas, M., Van Huynh, C. and Hoang Khanh Nguyen, L., 2019. Application of ordinary kriging and regression kriging method for soil properties mapping in hilly region of Central Vietnam. *ISPRS International Journal of Geo-Information*, 8(3), p.147.
- [12] Zhou, J., Xu, Y., Gu, X., Chen, T., Sun, Q., Zhang, S. and Pan, Y., 2023. High-Precision Mapping of Soil Organic Matter Based on UAV Imagery Using Machine Learning Algorithms. *Drones*, 7(5), p.290.
- [13] Iqbal, J., Xu, R., Halloran, H. and Li, C., 2020. Development of a multi-purpose autonomous differential drive mobile robot for plant phenotyping and soil sensing. *Electronics*, 9(9), p.1550.
- [14] Finegan, H., Jaffe, S., Leon, A., Lytle, K., Morgan, E., Greene, C., Meyer, A., Brinkman, B., De Wekker, S., Yochum, H. and Bezzo, N., 2019, April. Development of an autonomous agricultural vehicle to measure soil respiration. In *2019 Systems and Information Engineering Design Symposium (SIEDS)* (pp. 1-6). IEEE.
- [15] Ünal, I., Kabaş, Ö. and Sözer, S., 2020. Real-time electrical resistivity measurement and mapping platform of the soils with an autonomous robot for precision farming applications. *Sensors*, 20(1), p.251.
- [16] David, C.N.A., Yumol, J.V., Garcia, R.G. and Ballado, A.H., 2021, November. Swarm Robotics Application for Gathering Soil Samples. In *2021 IEEE 13th International Conference on Humanoid, Nanotechnology, Information Technology, Communication and Control, Environment, and Management (HNICEM)* (pp. 1-6). IEEE.
- [17] Łukowska, A., Tomaszuk, P., Dzierżek, K. and Magnuszewski, Ł., 2019, May. Soil sampling mobile platform for Agriculture 4.0. In *2019 20th International Carpathian Control Conference (ICCC)* (pp. 1-4). IEEE.
- [18] Barman, U. and Choudhury, R.D., 2019. Prediction of soil pH using smartphone based digital image processing and prediction algorithm. *Journal of Mechanics of Continua And Mathematical Sciences*, 14, pp.226-249.
- [19] Kasemi, R., Vincze, M. and Lammer, L., *EDGE SOIL: Low-Cost Soil Sensor and Edge AI Fusion in Agricultural Robotics*. Proceedings Austrian Robotics Workshop (ARW), 2023.
- [20] Krizhevsky, A., Sutskever, I. and Hinton, G.E., 2017. ImageNet classification with deep convolutional neural networks. *Communications of the ACM*, 60(6), pp.84-90.
- [21] - Zhang, X., Wu, F. and Li, Z., 2021. Application of convolutional neural network to traditional data. *Expert Systems with Applications*, 168, p.114185.
- [22] - Du, C., Wang, Y., Wang, C., Shi, C. and Xiao, B., 2020. Selective feature connection mechanism: Concatenating multi-layer CNN features with a feature selector. *Pattern Recognition Letters*, 129, pp.108-114.
- [23] Buck, R.P., Rondinini, S., Covington, A.K., Baucke, F.G.K., Brett, C.M., Camoes, M.F., Milton, M.J.T., Mussini, T., Naumann, R., Pratt, K.W. and Spitzer, P., 2002. Measurement of pH. Definition, standards, and procedures (IUPAC Recommendations 2002). *Pure and applied chemistry*, 74(11), pp.2169-2200.
- [24] Cohen, I., Huang, Y., Chen, J., Benesty, J., Benesty, J., Chen, J., Huang, Y. and Cohen, I., 2009. Pearson correlation coefficient. Noise reduction in speech processing, pp.1-4.
- [25] Lin, C., Mottaghi, S. and Shams, L., 2023. The effects of color and saturation on the enjoyment of real-life images. *Psychonomic Bulletin & Review*, pp.1-12.
- [26] Chicco, D., Warrens, M.J. and Jurman, G., 2021. The coefficient of determination R-squared is more informative than SMAPE, MAE, MAPE, MSE and RMSE in regression analysis evaluation. *PeerJ Computer Science*, 7, p.e623.
- [27] Hodson, T.O., Over, T.M. and Foks, S.S., 2021. Mean squared error, deconstructed. *Journal of Advances in Modeling Earth Systems*, 13(12), 2021.
- [28] Gallagher, P.A. and Herlihy, M., 1963. An evaluation of errors associated with soil testing. *Irish Journal of Agricultural Research*, pp.149-167.